Introduction to modelling cell mechanics and adhesion

Ulrich Schwarz
Heidelberg University
Institute for Theoretical Physics and BioQuant

Cell mechanics and adhesion

Animal cell in suspension

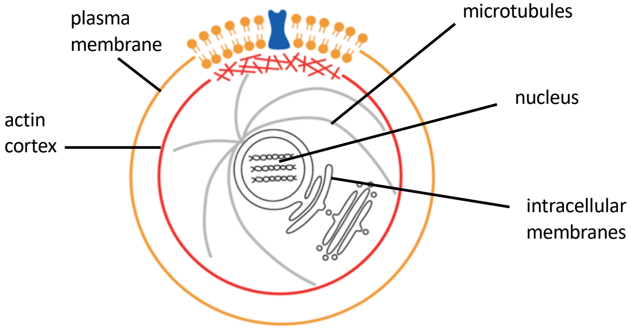

[Schwarz and Safran RMP 2013]

Animal cell in suspension reloaded

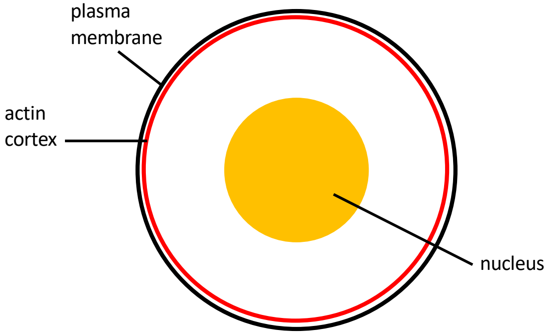

Cell spreading on homogeneous substrate

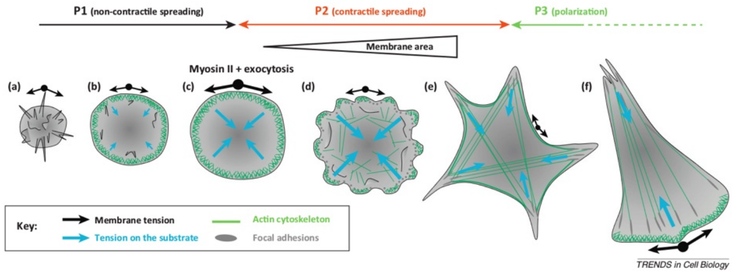

Actin polymerization pushes the leading edge forward and is balanced by membrane tension. The P1/P2-transition is characterized by activation of exocytosis and actomyosin contractility, leading to a reduction in membrane tension.

Gauthier et al., *Trends Cell Biol* 2012
Gauthier et al. PNAS 2011 and Pontes et al. JCB 2017

Cell in adhesion

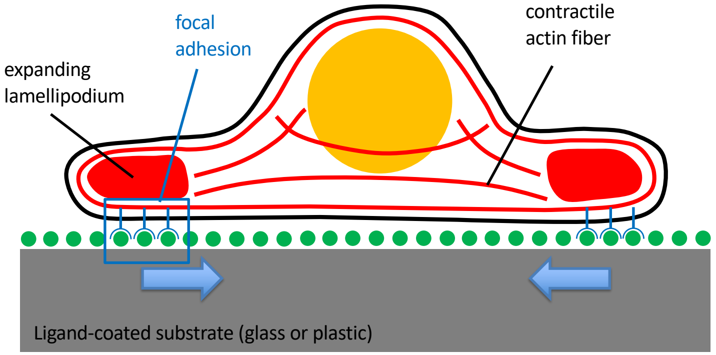

Cell contractility by myosin II motors

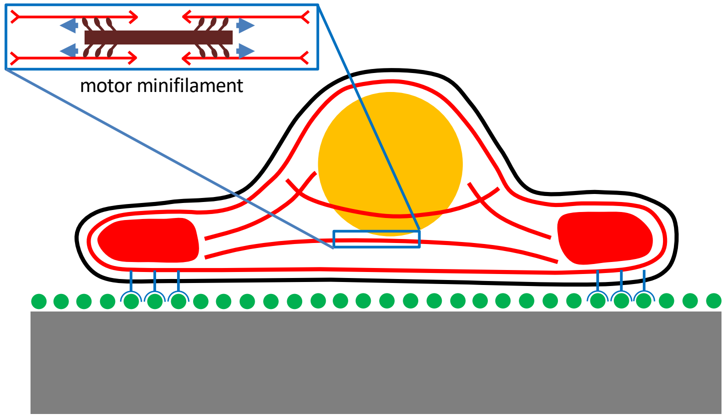

Network contraction by myosin II

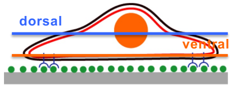

wildtype

myosin II inhibition

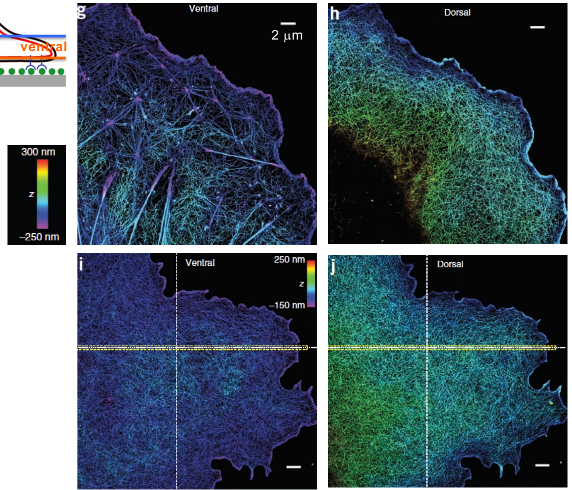

[Xu et al. Nature Methods 2012]

Cell organization and traction forces

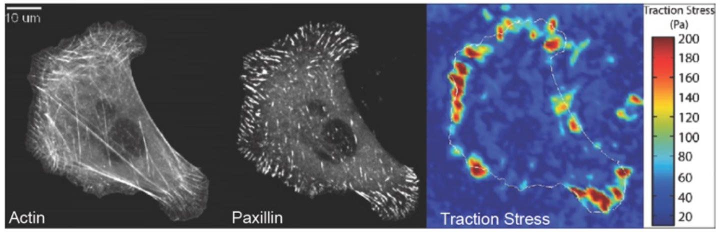

Cell forces can be measured by traction force microscopy and are strongly correlated with the organization of the actin cytoskeleton (stress fibers) and of the integrin-based adhesion sites (focal adhesions)

[Schwarz and Gardel JCS 2012]

Malaria-parasite moving in circle on soft elastic substrate

GFP-sporozoite on polyacrylamide substrate with two differently colored fluorescent beads

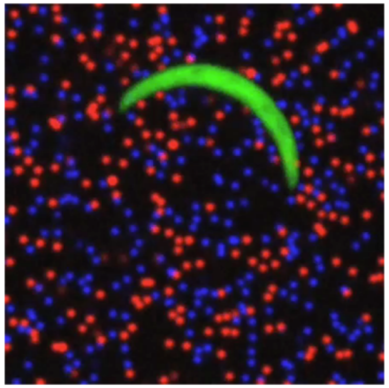

[Münter+ Cell Host Microbe 2009]

High resolution traction force microscopy

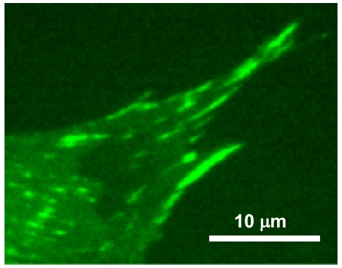

Fibroblast adhesion structures (paxillin) on 15 kPa polyacrylamide-substrate with two differently colored fluorescent nanobeads

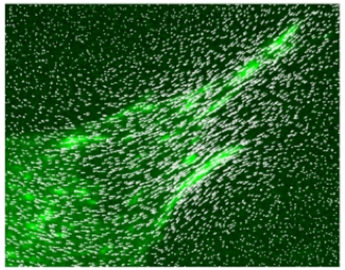

Displacement field extracted with correlation-based particle tracking velocimetry (mesh size 500 nm)

[Sabass+ BPJ 2008]

Regularized Fourier Transform Traction Cytometry (Reg-FTTC)

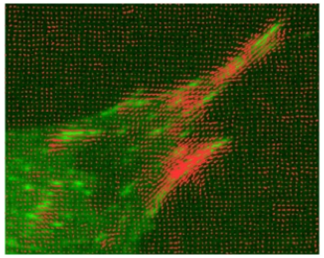

Traction vector field (spatial resolution 1 μm)

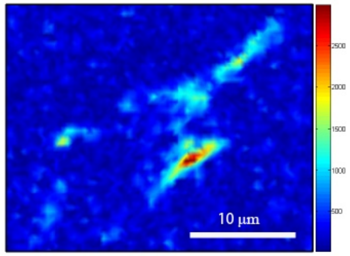

Traction magnitude (in Pa, resolution few 100 Pa)

The typical force per focal adhesion is 5 nN. With a typical FA size of μm^2, the typical stress is 5 kPa.

Rolling adhesion in shear flow

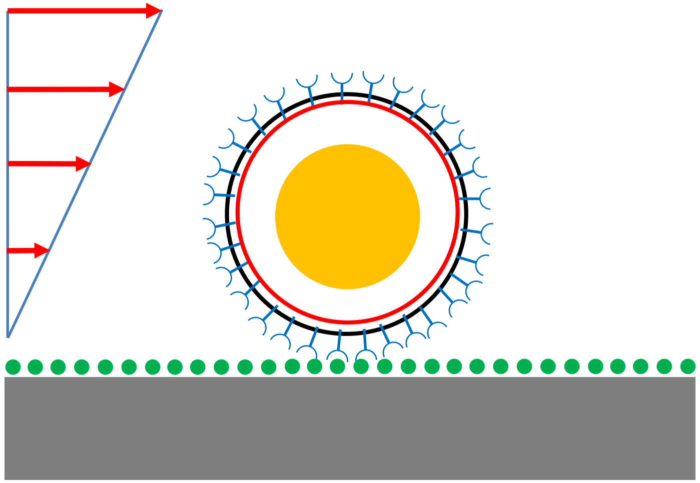

Intravital microscopy of neutrophil rolling

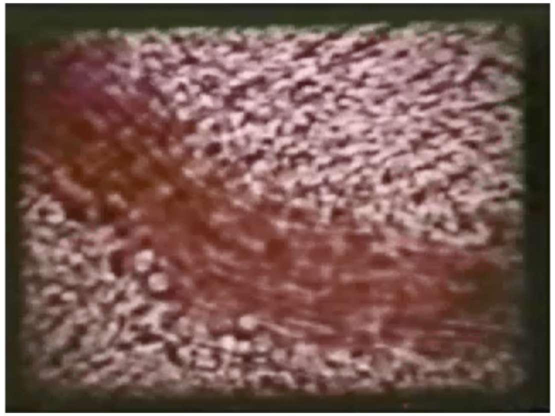

Simulating rolling adhesion

Six-dimensional Langevin equation for the sphere, mobility matrix from semi-analytical solution of the Stokes equation for sphere above a wall, master equation for bond dynamics

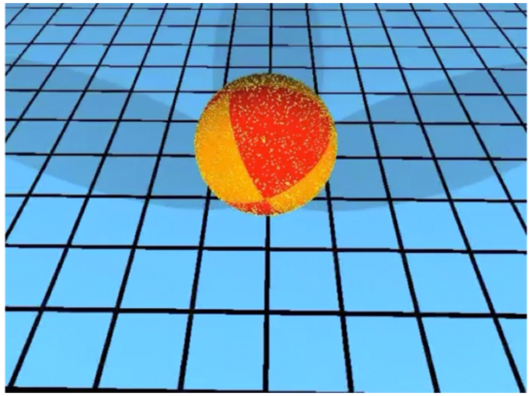

[Korn and Schwarz PRL 2006]

On-off kinetics of biomolecular bonds

- Receptors and ligands interact through weak interactions (screened electrostatics, van der Waals, hydrogen bonds), with typical binding energies of few k_BT and typical binding times of seconds
- We take the simplest possible approach: a two-state system (Z_2)
- Off-rates usually are increased by mechanical forces (*slip bonds*)
- On-rates depend strongly on the transport process that brings receptors and ligands together
- The asymmetry between association and dissociation implies that detailed balance is not necessarily obeyed

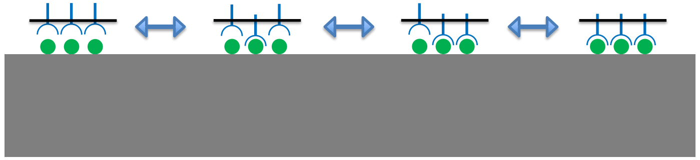

Modelling single bond dissociation

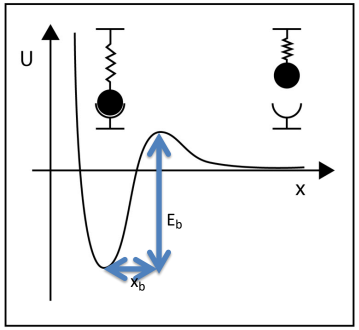

- can be modeled as escape over a transition state barrier (Kramers theory)
- typical time scale is seconds

$$k_0 = \frac{1}{t_D} e^{-\frac{E_b}{kT}} = 1\,\frac{1}{s}$$

with attempt time t_D = ns and energy barrier E_b = 20 kT

Dissociation under force

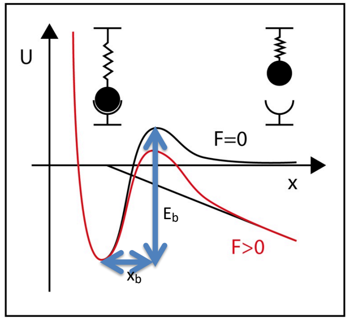

- force reduces barrier height E_b in proportion to distance x_b
- *Kramers-Bell-Evans equation*:

$$k = k_0 e^{F/F_b}$$

with F_b = kT / x_b = 10 pN for distance x_b = 4 A

Slip versus catch bonds

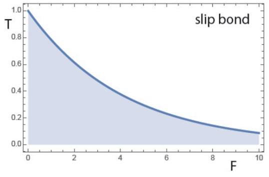

Lifetime (in s) decreases exponentially with force (in pN)

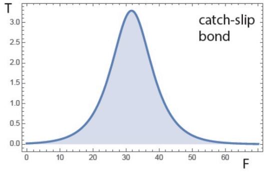

Lifetime (here for $\alpha_5\beta_1$-integrin-fibronectin) first increases and then decreases again with force

demonstrated in single molecule experiments for a wide range of ligand-receptor pairs

One-step master equation

- $p_i(t)$ probability that at time t exactly i bonds are closed $(0 \le i \le N_t)$

$$\frac{dp_i}{dt} = -[r_i + g_i]p_i + r_{i+1}p_{i+1} + g_{i-1}p_{i-1}$$

- rupture rate r_i from Kramers theory with load sharing, rebinding rate g_i force-independent

$$r_i = i e^{f/i}, \quad g_i = \gamma(N_t - i)$$

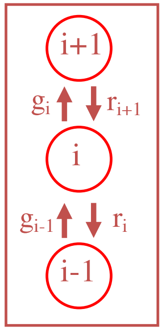

Dimensionless quantities: $f=F_b/F_0$ $\gamma=k_{on}/k_0$ $\tau=k_0t$

[Erdmann and Schwarz PRL 2004, JCP 2004]

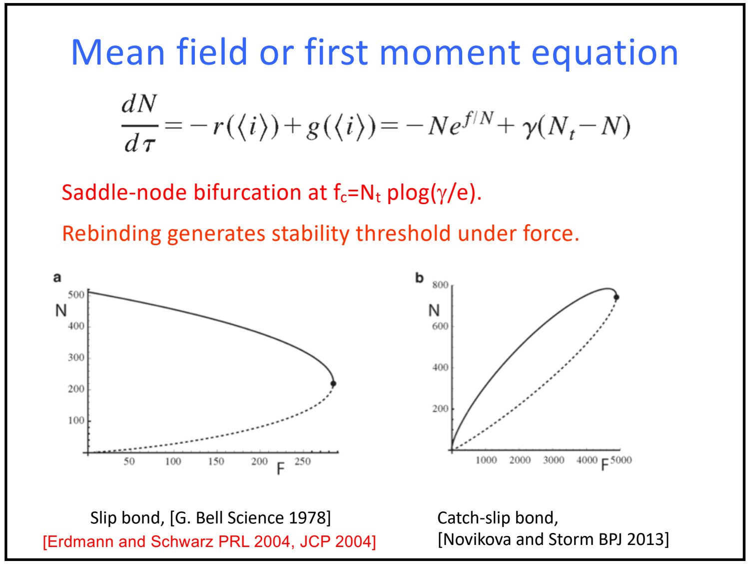

Mean field or first moment equation

$$\frac{dN}{d\tau} = -r(\langle i \rangle) + g(\langle i \rangle) = -Ne^{f/N} + \gamma(N_t - N)$$

Saddle-node bifurcation at $f_c = N_t\, p\log(\gamma/e)$.

Rebinding generates stability threshold under force.

Slip bond, [G. Bell Science 1978]
[Erdmann and Schwarz PRL 2004, JCP 2004]

Catch-slip bond,
[Novikova and Storm BPJ 2013]

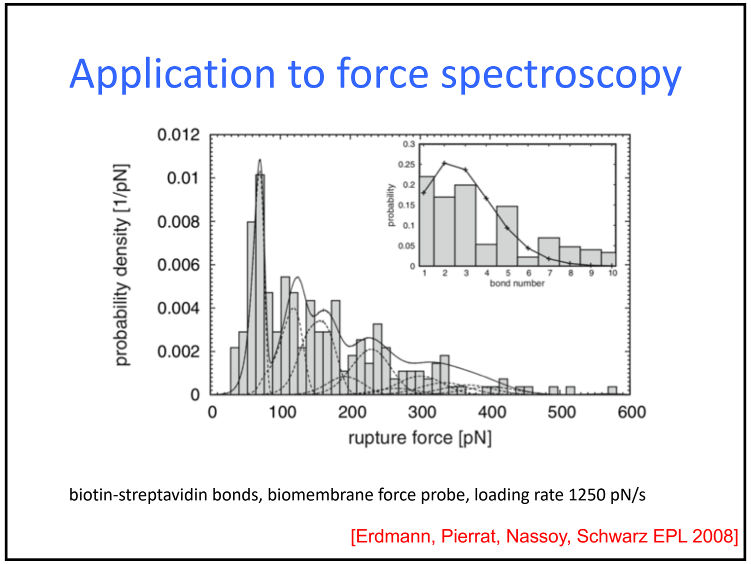

Application to force spectroscopy

biotin-streptavidin bonds, biomembrane force probe, loading rate 1250 pN/s

[Erdmann, Pierrat, Nassoy, Schwarz EPL 2008]

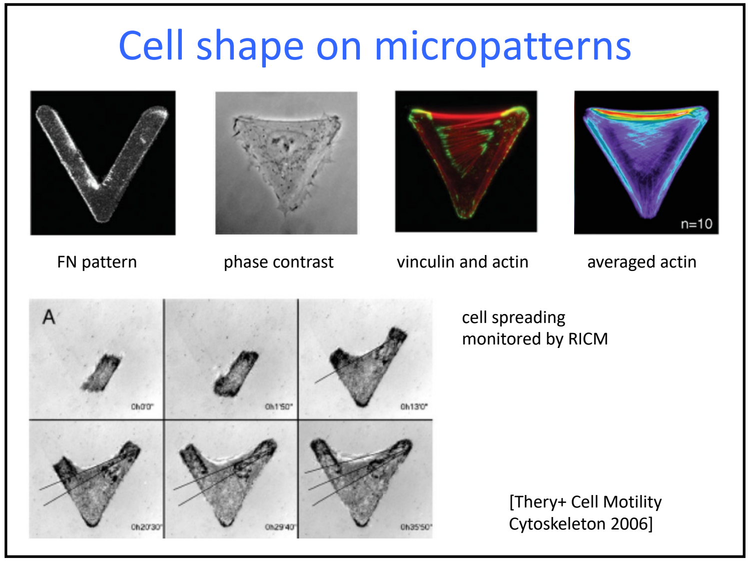

Cell shape on micropatterns

FN pattern

phase contrast

vinculin and actin

averaged actin

cell spreading
monitored by RICM

[Thery+ Cell Motility
Cytoskeleton 2006]

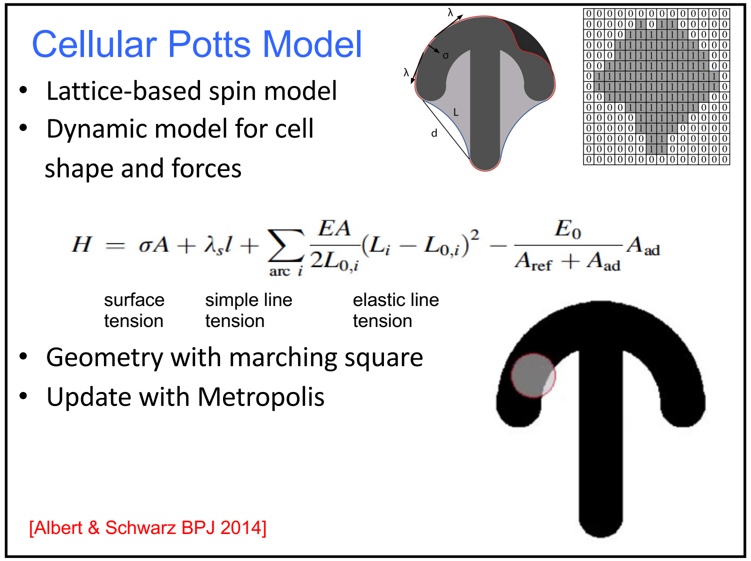

Cellular Potts Model

- Lattice-based spin model
- Dynamic model for cell shape and forces

$$H = \sigma A + \lambda_s l + \sum_{\mathrm{arc}\ i} \frac{EA}{2L_{0,i}}(L_i - L_{0,i})^2 - \frac{E_0}{A_{\mathrm{ref}} + A_{\mathrm{ad}}} A_{\mathrm{ad}}$$

surface
tension

simple line
tension

elastic line
tension

- Geometry with marching square
- Update with Metropolis

[Albert & Schwarz BPJ 2014]

Cell shape on different micropatterns

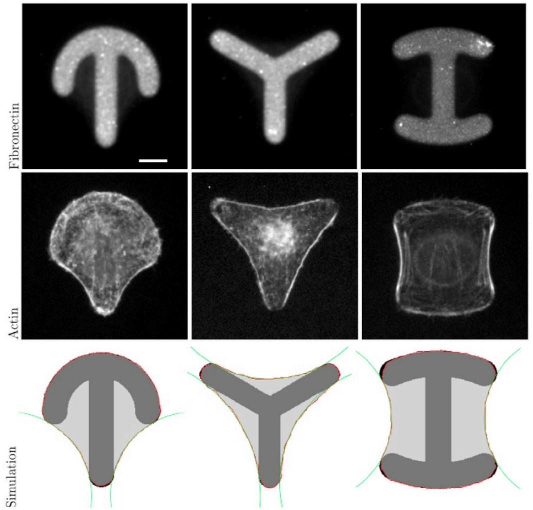

HeLa-cells, exps. by Starkuviene group

Laplace law for cell adhesion

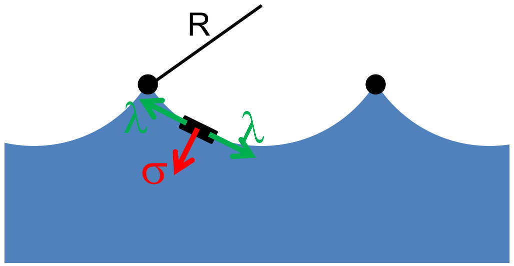

Force balance: $\sigma\vec{n} = \lambda \frac{d\vec{t}}{ds} = \frac{\lambda}{R}\vec{n} \quad \Rightarrow \quad R = \frac{\lambda}{\sigma}$

[Bar-Ziv+ PNAS 1999]

Force from Laplace law

$\lambda = R\sigma$

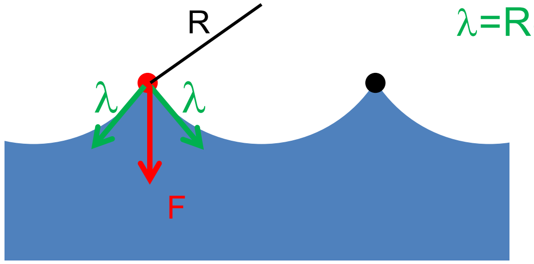

Only line tension λ contributes directly.
Only vectorial sum F is measured on the substrate.

[Bischofs, Schmidt & Schwarz PRL 2009]

Force from shape

[image Chen group]

- Surface tension σ is assumed to be constant
- Relative line tensions follow from $R_1/R_2=\lambda_1/\lambda_2$
- At each pillar, the two arc forces are summed up, resulting in a traction pattern
- A fit to the experimental results gives numbers for the force vectors
- Surface tension σ=2 nN/um

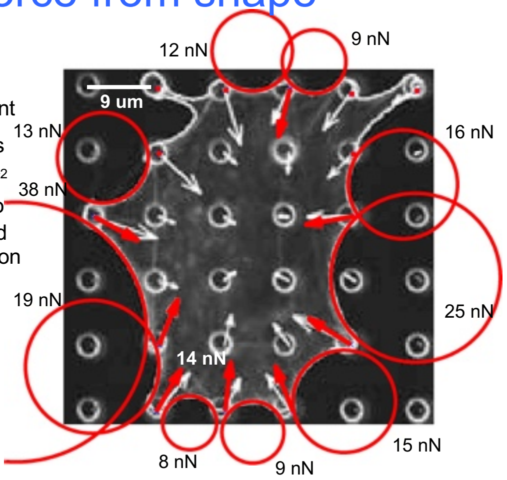

Cells in 3D spread in spatially heterogeneous matrices

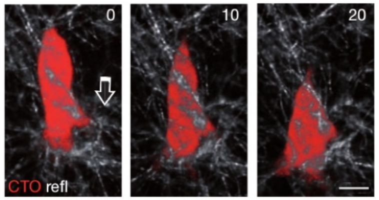

[Wolf et al. Nature Cell Biol 2007]
Cancer cells re-arrange collagen fibers and facilitate migration of followers

[Doyle and Yamada, *Exp Cell Res* 2016]
Fibroblasts in 3D collagen gels show robust adhesions

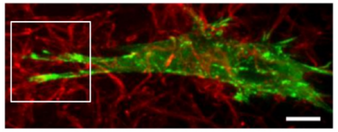

Cell organization in 3D gels

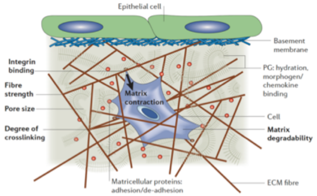

[Griffith and Swartz Nature Reviews MCB 2006]

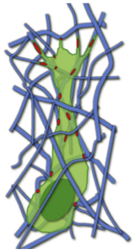

[Doyle and Yamada, *Exp Cell Res* 2016]

Cell shape in 3D scaffolds

[Brand+ Biophys 2017]

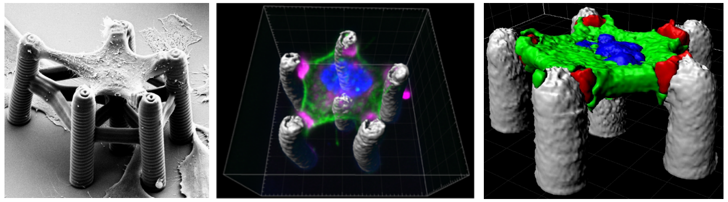

3D scaffold with one pillar moved out

Fluorescence image

Volume rendering with Imaris

Cells in open 3D scaffolds share most features of cells on 2D substrates. The difference to cells in 3D matrix is gradual, not fundamental.

Contractile surface model gives good agreement regarding shape

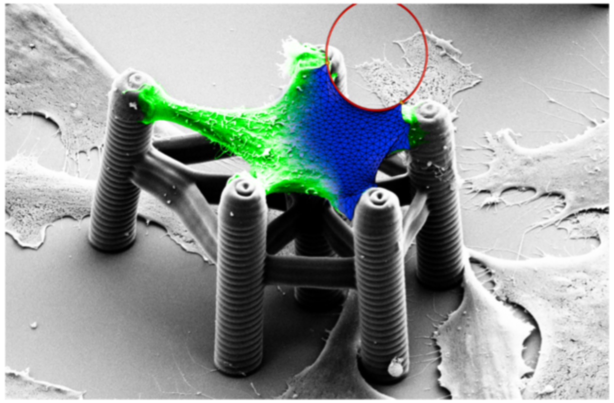

Summary first part

- Adhesion leads to complete remodelling of a cell: focal adhesions anchor it, lamellipodia drive the cell envelope outwards, actomyosin cortex and stress fibers stabilize it
- The cell senses the physical properties of its environment and strongly adapts to it
- Focal adhesions under force are only stable due to rebinding. The dynamics of biomolecular bonds allow cells to dynamically respond to changing conditions and at the same time to keep mechanical integrity
- To first approximation, cells are objects under strong tension and their shape is determined by the Laplace law

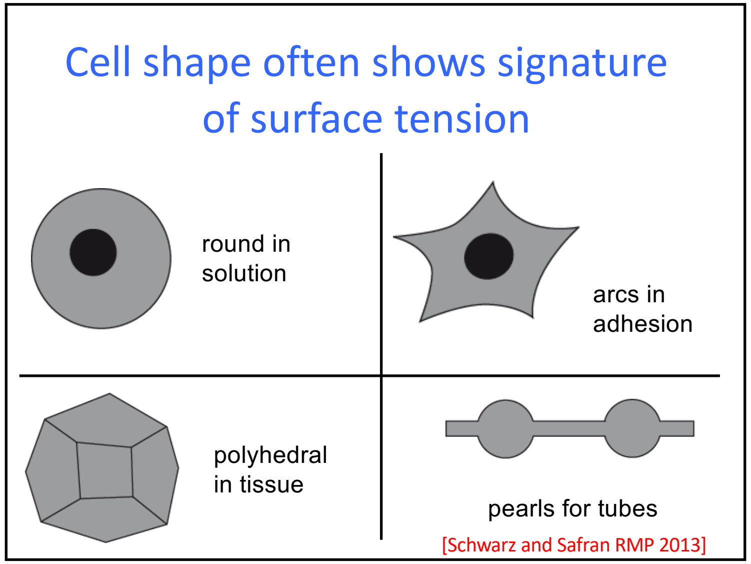

Cell shape often shows signature of surface tension

round in solution

arcs in adhesion

polyhedral in tissue

pearls for tubes

[Schwarz and Safran RMP 2013]

The red blood cell as model system for cell mechanics

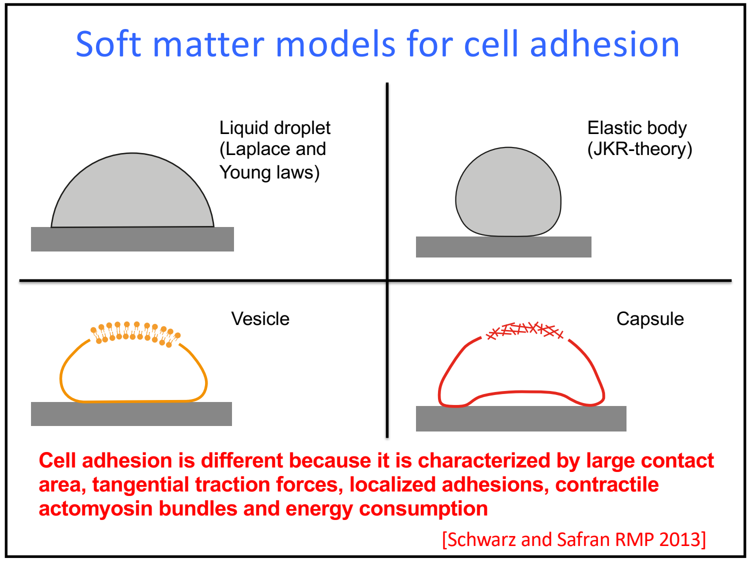

Soft matter models for cell adhesion

Liquid droplet (Laplace and Young laws)

Elastic body (JKR-theory)

Vesicle

Capsule

Cell adhesion is different because it is characterized by large contact area, tangential traction forces, localized adhesions, contractile actomyosin bundles and energy consumption

[Schwarz and Safran RMP 2013]

Breakdown of cell types in humans

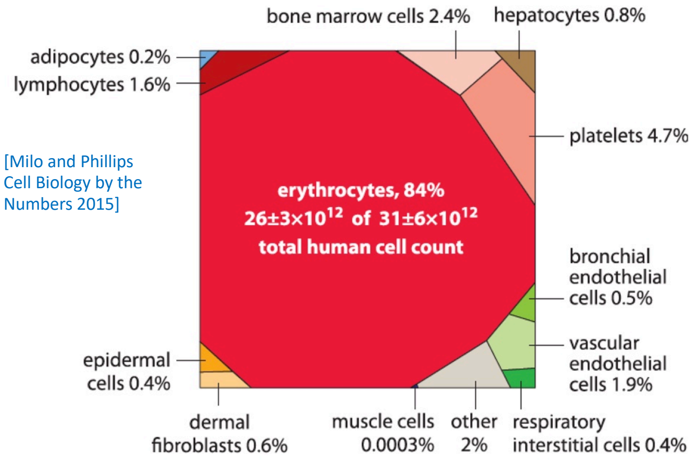

[Milo and Phillips Cell Biology by the Numbers 2015]

Blood cells

TYPE OF CELL	MAIN FUNCTIONS	TYPICAL CONCENTRATION IN HUMAN BLOOD (CELLS/LITER)
Red blood cells (erythrocytes)	transport O_2 and CO_2	5×10^{12}
White blood cells (leucocytes)		
Granulocytes		
Neutrophils (polymorphonuclear leucocytes)	phagocytose and destroy invading bacteria	5×10^{9}
Eosinophils	destroy larger parasites and modulate allergic inflammatory responses	2×10^{8}
Basophils	release histamine (and in some species serotonin) in certain immune reactions	4×10^{7}
Monocytes	become tissue macrophages, which phagocytose and digest invading microorganisms and foreign bodies as well as damaged senescent cells	4×10^{8}
Lymphocytes		
B cells	make antibodies	2×10^{9}
T cells	kill virus-infected cells and regulate activities of other leucocytes	1×10^{9}
Natural killer (NK) cells	kill virus-infected cells and some tumor cells	1×10^{8}
Platelets (cell fragments arising from *megakaryocytes* in bone marrow)	initiate **blood** clotting	3×10^{11}

Humans contain about 5 liters of **blood**, accounting for 7% of body weight. Red **blood** cells constitute about 45% of this volume and white **blood** cells about 1%, the rest being the liquid **blood** plasma.

Alberts MBoC

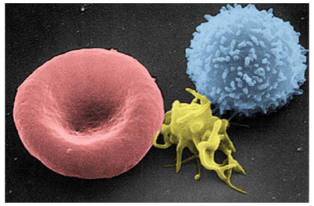

Red blood cell, platelet, white blood cell (from wikipedia)

3×10^{13} red blood cells in each of us, lifetime 120 days

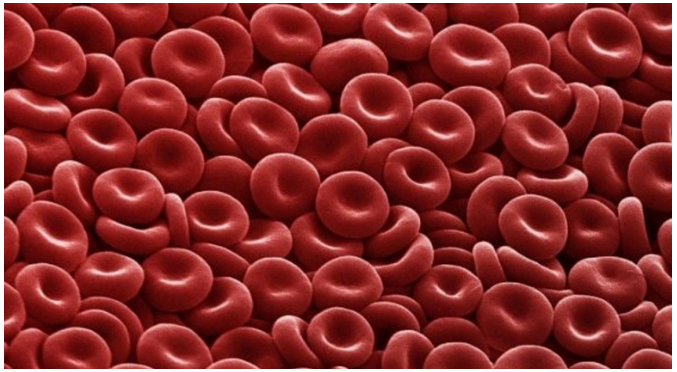

Fig 1. Scanning electron microscope (SEM) image of a RBC population having different morphology stages of stomatocytosis and echinocytosis.

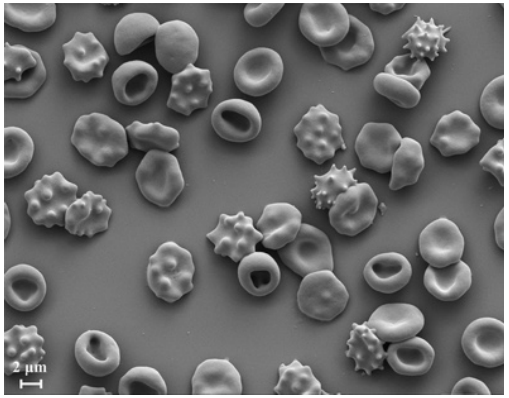

Geekiyanage NM, Balanant MA, Sauret E, Saha S, Flower R, et al. (2019) A coarse-grained red blood cell membrane model to study stomatocyte-discocyte-echinocyte morphologies. PLOS ONE 14(4): e0215447. https://doi.org/10.1371/journal.pone.0215447
https://journals.plos.org/plosone/article?id=10.1371/journal.pone.0215447

PLOS ONE

Structure of the RBC-envelope

Composite of lipid bilayer and spectrin skeleton

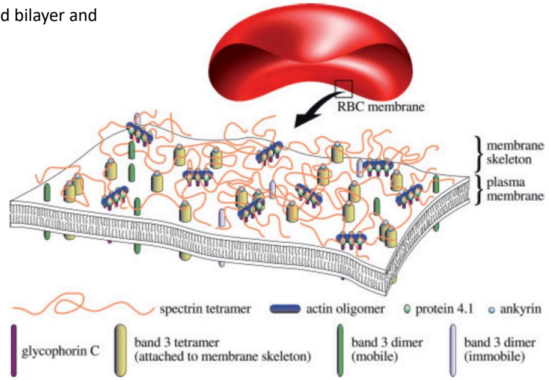

Very important: no motors, no contractility, no adhesion

Helfrich bending Hamiltonian for biomembranes

$$H = \int dA\{\sigma + 2\kappa(H - c_0)^2\}$$

- $H = (1/R_1 + 1/R_2)/2$ mean curvature
- c_0 spontaneous curvature for asymmetric bilayers
- σ surface tension around 10^{-4} N/m
- κ bending rigidity around 25 k_B T

Euler-Lagrange equations: $p + 2\sigma H - 2\kappa\left(2H\left(H^2 - K\right) - \Delta H\right) = 0$

can be solved by ODE-shooting for axisymmetric shapes

Shape diagram for vesicles

Bending Hamiltonian, Euler-Langrange equations,
the only parameter is the reduced volume $v=V/(4\pi/3\ R^3)$, $A=4\pi R^2$

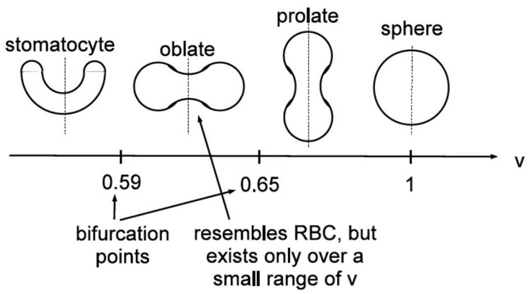

Artificial vesicles with pure bilayers are studied as simplest cell models

Experimentally one observes different shape transitions, e.g. prolate to bud

For given area and volume, the only relevant parameter is reduced volume

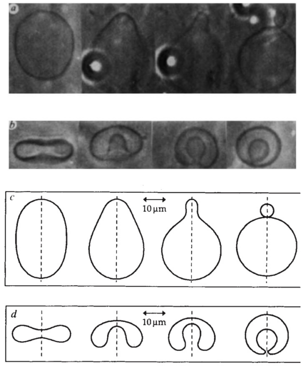

FIG. 1 Shape transformations of free vesicles induced by a change i temperature[4]. *a, c,* Expulsion of a small vesicle from a larger one (budding *b, d,* Inverse budding ('endocytosis') via the transformation from a discocyt to a stomatocyte. The shapes are axisymmetric with respect to the broke line.

Lipowsky review Nature 1991

Shape diagram for the area difference elasticity (ADE) model

Original paper: Ling Miao, Udo Seifert, Michael Wortis, and Hans-Günther Döbereiner, PRE 1994

$$\mathcal{H} = 2\kappa \int dA\, H^2 + \frac{\alpha}{2}(\Delta A - \Delta A_0)^2$$

Shape diagram depends on two variables: preferred area difference and reduced volume

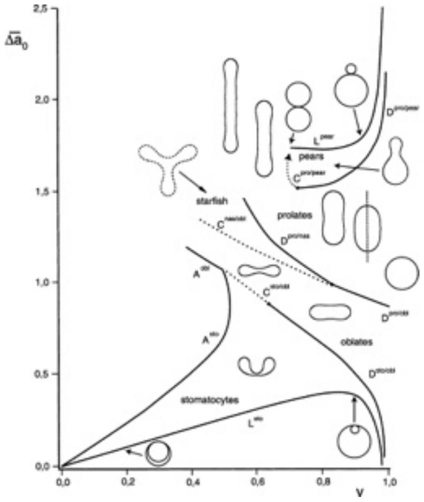

Elastic surface Hamiltonian for RBCs

Helfrich bending Hamiltonian for plasma membrane as above

Elastic Hamiltonian for spectrin-actin-network:

$$\mathcal{H} = \frac{K_\alpha}{2} \int dA \left(\alpha^2 + \alpha_3 \alpha^3 + \alpha_4 \alpha^4\right) + \mu \int dA \left(\beta + b_1 \alpha\beta + b_2 \beta^2\right)$$

with $\alpha = \lambda_1 \lambda_2 - 1,\ \beta = \frac{1}{2}\left(\frac{\lambda_1}{\lambda_2} + \frac{\lambda_2}{\lambda_1} - 2\right)$ strain invariants

Euler-Lagrange equations very challenging, usually solved by direct surface minimization

Shapes of the red blood cell

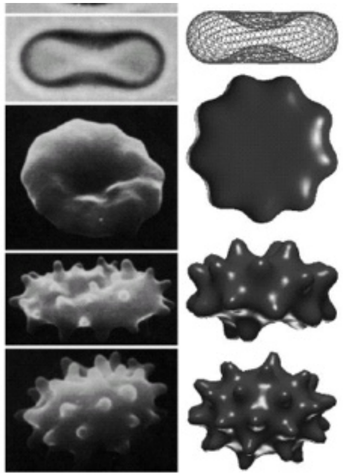

discocyte

phospholipids

cholesterol

anionic lipids

high salt/pH

ATP depletion

larger ΔA

echinocyte

[Lim et al. PNAS 2002]

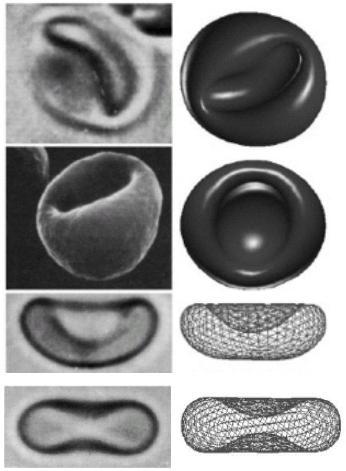

stomatocyte

cholesterol depletion

cationic lipids

low salt/pH

smaller ΔA

discocyte

Full model for RBC shape

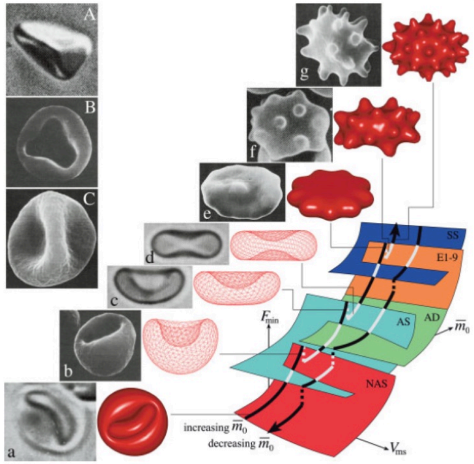

[Lim, Wortis, Mukhopadhyay review 2008]

Most recent work comparing different model predictions with experiments

RESEARCH ARTICLE

A coarse-grained red blood cell membrane model to study stomatocyte-discocyte-echinocyte morphologies

Nadeeshani Maheshika Geekiyanage[1], **Marie Anne Balanant**[1,2], **Emilie Sauret**[1]*, **Suvash Saha**[3], **Robert Flower**[2], **Chwee Teck Lim**[4,5,6], **YuanTong Gu**[1]*

1 School of Chemistry, Physics and Mechanical Engineering, Queensland University of Technology (QUT), Brisbane, Queensland, Australia, **2** Research & Development, Australian Red Cross Blood Service, Brisbane, Queensland, Australia, **3** University of Technology Sydney (UTS), Ultimo, New South Wales, Australia, **4** Department of Biomedical Engineering, Faculty of Engineering, National University of Singapore, Singapore, **5** Biomedical Institute for Global Health Research and Technology, National University of Singapore, Singapore, **6** Mechanobiology Institute, National University of Singapore, Singapore

* emilie.sauret@qut.edu.au (ES); yuantong.gu@qut.edu.au (YG)

Check for updates

OPEN ACCESS

Citation: Geekiyanage NM, Balanant MA, Sauret E, Saha S, Flower R, Lim CT, et al. (2019) A coarse-grained red blood cell membrane model to study stomatocyte-discocyte-echinocyte morphologies. PLoS ONE 14(4): e0215447. https://doi.org/10.1371/journal.pone.0215447

Editor: Krishna Garikipati, University of Michigan, UNITED STATES

Received: January 15, 2019

Accepted: April 2, 2019

Published: April 19, 2019

Abstract

An improved red blood cell (RBC) membrane model is developed based on the bilayer coupling model (BCM) to accurately predict the complete sequence of stomatocyte-discocyte-echinocyte (SDE) transformation of a RBC. The coarse-grained (CG)–RBC membrane model is proposed to predict the minimum energy configuration of the RBC from the competition between lipid-bilayer bending resistance and cytoskeletal shear resistance under given reference constraints. In addition to the conventional membrane surface area, cell volume and bilayer-leaflet-area-difference constraints, a new constraint: total-membrane-curvature is proposed in the model to better predict RBC shapes in agreement with experimental observations. A quantitative evaluation of several cellular measurements including length, thickness and shape factor, is performed for the first time, between CG-RBC model predicted and three-dimensional (3D) confocal microscopy imaging generated RBC shapes at equivalent reference constraints. The validated CG-RBC membrane model is then employed to investigate the effect of reduced cell volume and elastic length scale on SDE transformation, to evaluate the RBC deformability during SDE transformation, and to identify the most probable RBC cytoskeletal reference state. The CG-RBC membrane model can predict the SDE shape behaviour under diverse shape-transforming scenarios, in-vitro RBC storage, microvascular circulation and flow through microfluidic devices.

Fig 4. Summary of estimated cell surface area (Aex), cell volume (Vex), bilayer-leaflet-area-difference (ΔAex), total-membrane-curvature (Cex) and equivalent reduced cell volume (vex) for the experimentally observed discocyte, echinocyte I, echinocyte II and echinocyte III RBC shapes.

Shape Classification		Experimental Observations (Confocal Microscopy Imaging)	Experimental Observations (Triangulated Surface Mesh)	A^{ex} (μm²)	V^{ex} (μm³)	$\Delta A^{ex}/A^{ex}$ (%)	C^{ex}/A^{ex} (%)	v^{ex}
Discocyte				145.046	101.623	0.124	0.244	0.619
Echinocyte	I	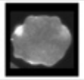		129.634	82.052	0.138	0.298	0.591
	II			140.054	91.767	0.143	0.411	0.589
	III	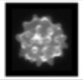		131.450	91.547	0.161	0.624	0.646

Geekiyanage NM, Balanant MA, Sauret E, Saha S, Flower R, et al. (2019) A coarse-grained red blood cell membrane model to study stomatocyte-discocyte-echinocyte morphologies. PLOS ONE 14(4): e0215447. https://doi.org/10.1371/journal.pone.0215447
https://journals.plos.org/plosone/article?id=10.1371/journal.pone.0215447

PLOS | ONE

Importance of reference shape

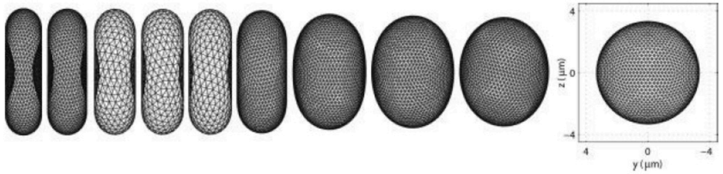

Spectrum of possible reference shapes for RBC skeleton ranging from discocyte (flaccid, left) to sphere (turgid, right). Because experiments can not clarify this point, computation is essential.

[Lim, Wortis, Mukhopadhyay review 2008]

Importance of non-linear elasticity

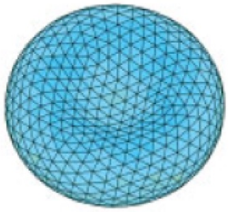
discocyte

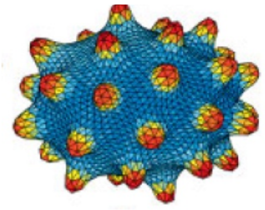
echinocyte

Color code for stretch ratio alpha: echinocytes are highly strained.

[Lim, Wortis, Mukhopadhyay review 2008]

Stretching RBCs with an optical tweezer

Computational model with roughly 20.000 vertices

Stretching force given in pico Newton

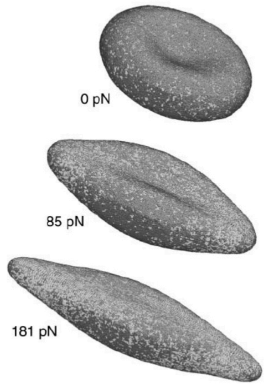

[Li+ BPJ 2005]

RBCs in shear flow

- Single fluid vesicles and RBCs in shear flow undergo tank-treading (TT) and tumbling (TB) motions
- With increasing shear rate, they undergo a TT-TB transition

$$\begin{pmatrix} 0 & \dot\gamma \\ 0 & 0 \end{pmatrix} = \begin{pmatrix} 0 & \dot\gamma/2 \\ \dot\gamma/2 & 0 \end{pmatrix} + \begin{pmatrix} 0 & \dot\gamma/2 \\ -\dot\gamma/2 & 0 \end{pmatrix}$$

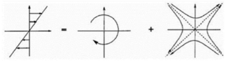

linear shear = rotation + elongation (Geislinger + Franke 2014)

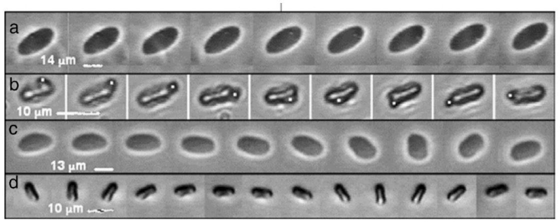

Vesicle TT

RBC TT

Vesicle TB

RBC TB

Abkarian PRL 2007 and Soft Matter 2008

RBC shape transition at high shear

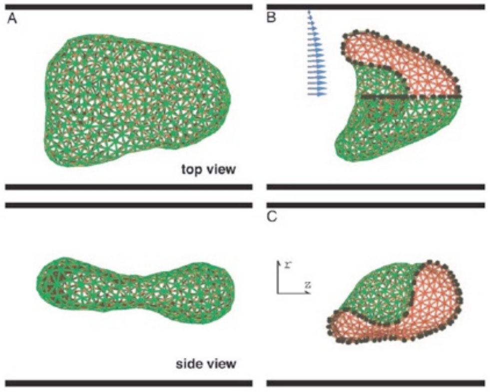

parachute

slipper

[Noguchi and Gompper PNAS 2005]

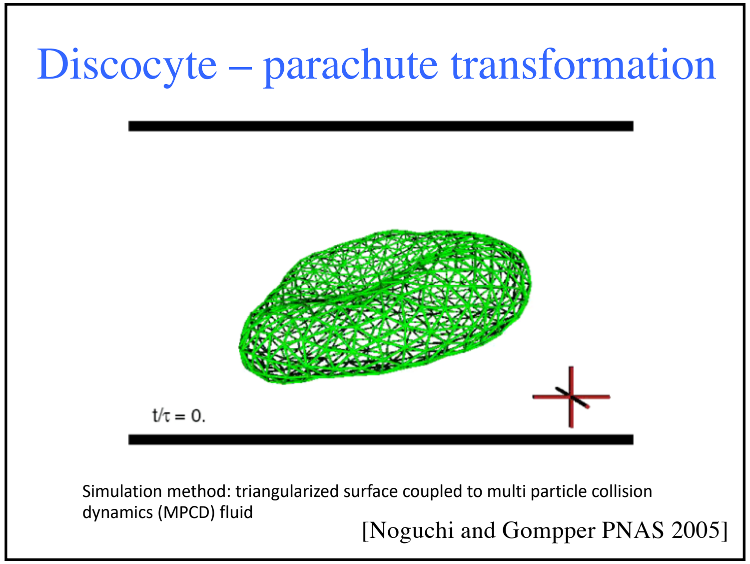

Discocyte – parachute transformation

Simulation method: triangularized surface coupled to multi particle collision dynamics (MPCD) fluid

[Noguchi and Gompper PNAS 2005]

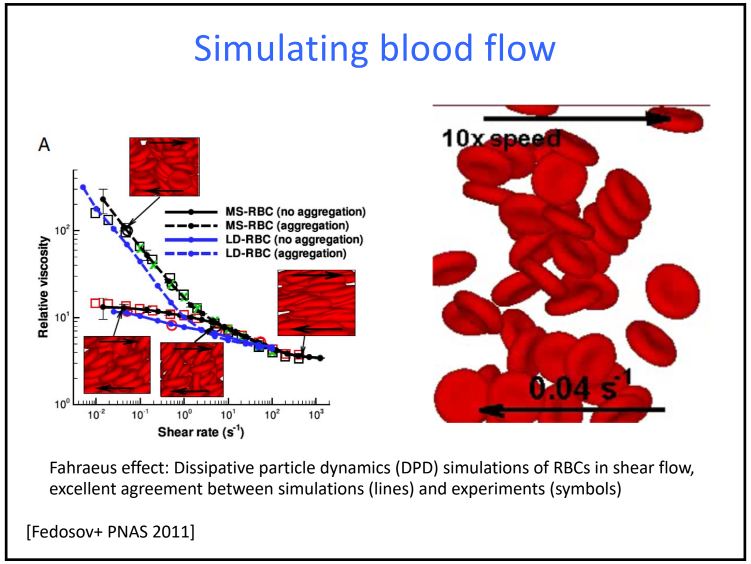

Simulating blood flow

Fahraeus effect: Dissipative particle dynamics (DPD) simulations of RBCs in shear flow, excellent agreement between simulations (lines) and experiments (symbols)

[Fedosov+ PNAS 2011]

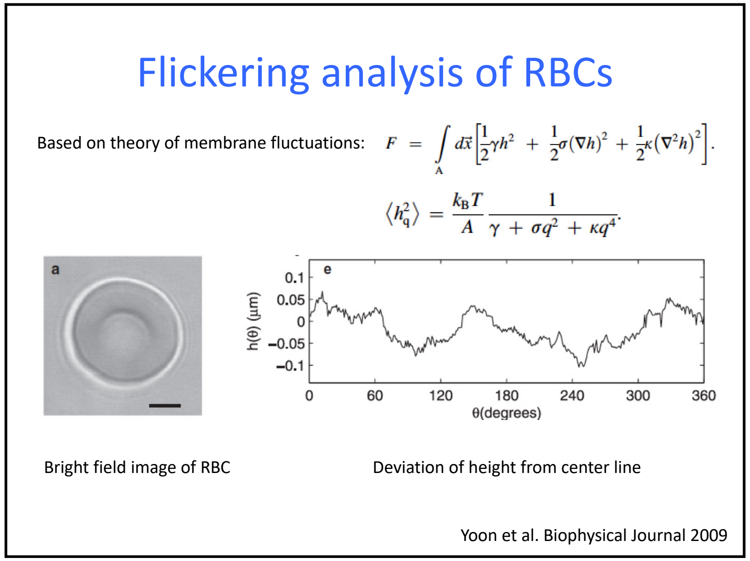

Flickering analysis of RBCs

Based on theory of membrane fluctuations:

$$F = \int_A d\vec{x}\left[\frac{1}{2}\gamma h^2 + \frac{1}{2}\sigma(\nabla h)^2 + \frac{1}{2}\kappa(\nabla^2 h)^2\right].$$

$$\langle h_q^2\rangle = \frac{k_B T}{A}\frac{1}{\gamma + \sigma q^2 + \kappa q^4}.$$

Bright field image of RBC

Deviation of height from center line

Yoon et al. Biophysical Journal 2009

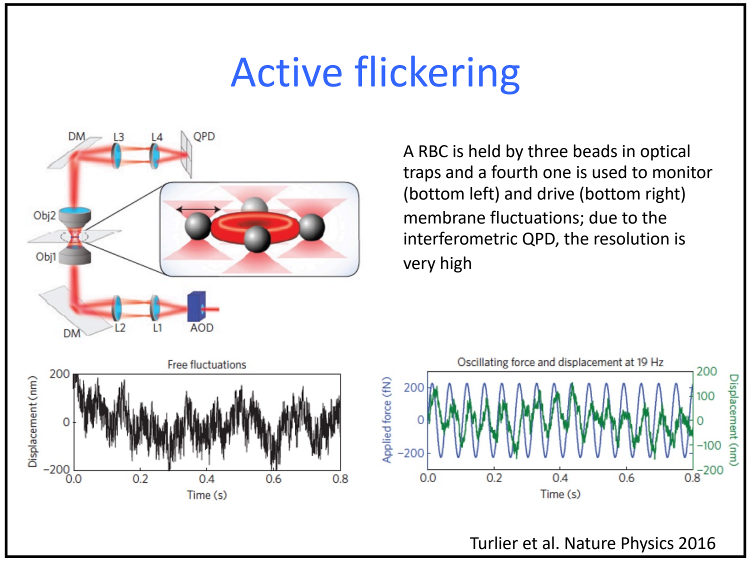

Active flickering

A RBC is held by three beads in optical traps and a fourth one is used to monitor (bottom left) and drive (bottom right) membrane fluctuations; due to the interferometric QPD, the resolution is very high

Turlier et al. Nature Physics 2016

Violation of the fluctuation-dissipation theorem

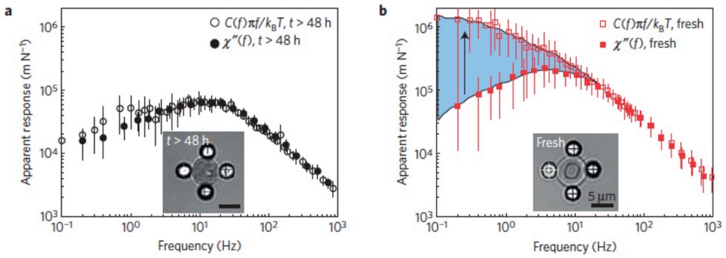

Passive RBC (ATP-): fluctuations and dissipation agree according to the FDT

$$\langle b^2(\omega)\rangle = \frac{2k_BT}{\omega}\chi''(\omega)$$

Active RBC (ATP+): at low frequencies, the active fluctuations dominate over the passive dissipation

Summary second part

- RBCs lack actomyosin contractility and adhesion
- Their biconcave shape is explained by bending energy at reduced volume around v=0.61
- The spectrin-actin cytoskeleton stabilizes this shape and prevents budding
- RBCs in shear flow assume many different shapes (e.g. parachutes)
- Membrane flickering has a strong active component